# Effect of rotation on internal dynamics and phase-space structure of rare-gas trimers

E. D. Belega,[1] D. N. Trubnikov,[1] and Lawrence L. Lohr[2]
[1]*Department of Chemistry, Moscow State University, Leninskiye Gory, Moscow 109899, Russia*
[2]*Department of Chemistry, University of Michigan, Ann Arbor, Michigan 48109-1055*
(Received 30 November 1998; revised manuscript received 9 October 2000; published 20 March 2001)

The effect of total rotational angular momentum on the stochastic characteristics of the internal motion of rare-gas trimers has been studied by the molecular-dynamics method. Results presented for the argon trimer described in a two-parameter phase space characterized by fixed values of the total energy and angular momentum provide insight into the separation of chaotic from regular motions of the system. An important feature of the phase-space structure is that the volume filled by regular trajectories for fixed total energy of the system is not a monotonic function of its total angular momentum. The chaotic motions are characterized by a strong coupling between potential- and kinetic-energy contributions that is not observed for the regular motions.

DOI: 10.1103/PhysRevA.63.043203 PACS number(s): 36.40.−c, 05.45.−a

## I. INTRODUCTION

Over the past two decades a main focus of the study of van der Waals clusters has been the characterization of those properties that are similar to, and those that are different from, the properties of bulk materials. Potential-energy surfaces have been calculated, global and local minima as well as saddle points located, and the relationship between structure and internal dynamics studied [1] within the framework of the theory of quasiphase transitions for clusters. Short-time averages of dynamic variables and such stochastic parameters as the maximum Lyapunov exponent [2–5] or Kolmogorov entropy (the sum of positive Lyapunov numbers) have been widely used [6–8] to characterize the internal dynamics and phase-space structures of clusters. Zero values of these parameters are a signature of regular motion or rigidity of the systems.

The simplest rare-gas cluster, namely the trimer, has been used to reveal the relationship between the time behavior of stochastic parameters and the structure of its potential-energy surface. For $Ar_3$ with zero angular momentum and with a fixed total energy slightly higher than that required to allow passage across the linear saddle point the phase space is split into regions with differing degrees of chaotic motion [3,4], depending on the set of microcanonical initial conditions. The distributions of Lyapunov exponents also depend on the initial conditions and do not converge for infinite time [4]. The Kolmogorov entropy does not increase monotonically with energy, but rather it reaches a plateau and then drops once the cluster has sufficient energy to explore the linear saddle region [6]. Low chaotic trajectories are associated with the saddle region (linear structure for the trimer), which channels neighboring trajectories, thus reducing their divergence and reducing the Kolmogorov entropy and the degree of chaos. It was also noted that saddle regions can decouple vibrational modes and induce temporary and approximately quasiperiodic behavior [8]. Applying stochastic theory to the dynamics of molecules such as $SO_2$ and $O_3$ [9], it was found that their phase spaces consist of chaotic trajectories differing markedly in the value of their maximum Lyapunov exponent for energies above the critical energy, reflecting a partition of the chaotic component of motion. The ''structure of chaos'' connected with the partition of the stochastic component was also investigated for $Ar_4$ [10]. The partition of the chaotic component leads to the existence of different times for energy redistribution between internal degrees of freedom. This property nearly disappears with increasing energy for dynamical systems with anharmonic potentials, as expected from the Kolmogorov-Arnol'd-Moser (KAM) theorem [11].

Nearly all of the studies cited above were carried out as a function of energy only, not taking into account the influence of molecular rotation. One exception was a study [10] of the role of rotational motion in the chaotic region of the phase space for the tetramer $Ar_4$. Specifically studied was the partition of internal energy between internal degrees of freedom as a function of rotational angular momentum. No differences in stochastic parameters were found in comparison to those of a rotationless cluster.

A detailed dynamical simulation of rotating $Ar_{13}$ [12] showed that its internal dynamics and rigidity is not uniquely defined by its total energy but instead strongly depends on the initial state of the cluster, and more specifically on the initial distribution of momenta among the internal degrees of freedom. The maximum Lyapunov exponent for the system was found to behave nonmonotonically with increasing total energy.

It is reasonable that increasing rotational angular momentum for fixed total energy will tend to regularize the motion, leading to the occurrence of nonchaotic trajectories, by lowering the vibrational kinetic energy and thus altering the phase-space structure. This assumption is supported by results reported for rotating $HD_2^+$ [13], for which the consequences of switching on rotation include centrifugal stretching, which reduces chaos by stiffening of the bonds, Coriolis forces, which increase nonlinearity, and tumbling, which is the motion of the angle between the angular momentum vector and the normal to the molecular plane and which leads to an increase in stochasticity but is limited by energy conservation. Thus at high angular momentum but relatively low energy, the degree of chaos is reduced and approaches a minimum in the limit of a centrifugally distorted but nonvi-

 

brating cluster. This minimum is zero for asymmetric tops and oblate symmetric tops but is nonzero for prolate symmetric tops and spherical tops due to the chaos associated with tumbling in a laboratory frame.

Our earlier work [14] on the phase space structure of rotating $Ar_3$ at a total energy corresponding to one-half of the well depth, an energy thus above that of linear $Ar_3$ but below that of $Ar_2$ and Ar fragments, showed the partition of the phase space into regions of regular and chaotic motion as well as a partition of the chaotic component into portions with differing maximum Lyapunov exponents and differing shapes of the autocorrelation function of atomic momentum on an axis normal to the angular momentum **M**. The nonmonotonic character of the regular fraction was explained in terms of the regularizing influence of the linear configuration and the freezing of energy in rotational degrees of freedom when $M=|\mathbf{M}|$ approaches its maximum possible value for a given total energy.

We also studied [15] the phase-space structure of $Ar_4$ with nonzero angular momentum at energies above that corresponding to a planar configuration. We found that for a given energy there is a critical $M_c=|\mathbf{M}_c|$ for the structural transformation in which one atom passes through the plane of the three others, thus inverting the tetrahedron. For values of $M$ greater than $M_c$ the transformation is impossible and the phase space is partitioned into two nonoverlapping regions. More recent studies by Yertsever *et al.* [16–18] showed that for rotating $Ar_3$ initially generated as an equilateral triangle the maximum Lyapunov exponent has a nonmonotonic behavior with increasing total energy but decreases with increasing angular momentum.

In this paper we employ molecular dynamics to investigate the effect of rotation on the phase-space structure of rare-gas trimers. In Sec. II we describe the details of the method including the numerical scheme for calculating stochastic parameters and distributions of the dynamical variables. In Sec. III we discuss the maximum Lyapunov exponents, the autocorrelation function for the momentum of an atom on an axis normal to the angular momentum **M**, and distribution functions for the interatomic distances and for potential and kinetic energy contributions for various $M$. In Sec. IV we discuss these results in the context of future research plans.

## II. METHOD

Consider the rotating $Ar_3$ cluster as a bound state of the classical Hamiltonian

$$H=\sum_{i=1}^{3}\frac{\mathbf{p}_i^2}{2m}+4U_0\sum_{i>j}\left[\left(\frac{\alpha}{r_{ij}}\right)^{12}-\left(\frac{\alpha}{r_{ij}}\right)^{6}\right], \qquad (1)$$

where the potential energy is taken in a pairwise additive Lennard-Jones form, $\mathbf{p}_i$ is the momentum of the $i$th atom (each of mass $m$), $r_{ij}$ is the interparticle distance $|\mathbf{r}_i-\mathbf{r}_j|$, $\mathbf{r}_i$ is the position of the $i$th atom, $U_0$ is the diatomic well depth, and $\alpha$ is the diatomic collision diameter. The familiar [19] parameters $\alpha$, $U_0$, and $m$ are taken as dimensionless, with $(m\alpha^2/U_0)^{1/2}$ as the unit of time. The nonrotating cluster has a minimum energy of $-3.0$ and an equilateral triangular structure with an equilibrium edge length equal to the diatomic equilibrium separation of $2^{1/6}\alpha$.

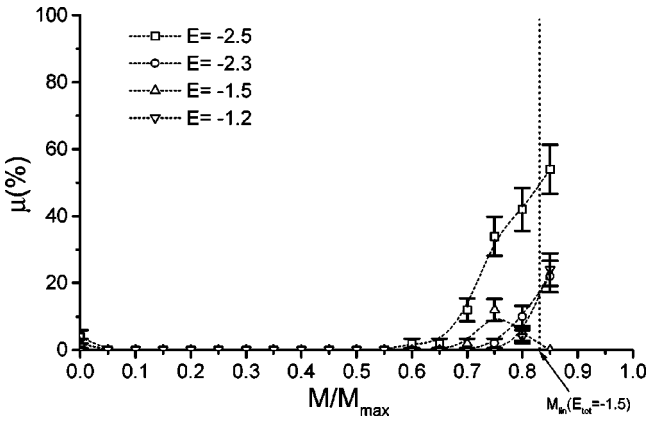


FIG. 1. Dependence on the normalized angular momentum $M(E)/M_{\max}(E)$ of the percentage $\mu$ of phase space filled by regular trajectories for four different values of the total internal energy of $Ar_3$. The dashed vertical line corresponds to the normalized maximum value of $M_{\rm lin}$ for the linear trimer with $E_{\rm tot}=-1.5$. The energy unit is the natural unit corresponding to the diatomic well depth of 99.45 $\mathrm{cm}^{-1}$.

We have used molecular dynamics to study the phase-space structure of rotating $Ar_3$ as a function of two parameters, namely the total energy $E_{\rm tot}$ and the total angular momentum. A microcanonical ensemble of initial conditions was formed by straightforward sampling from points distributed randomly and uniformly in coordinate space such that the potential energy $U\leqslant E_{\rm tot}$ and in momentum space such that the kinetic energy $E_{\rm kin}=E_{\rm tot}-U$. Further, the points were selected from the angular momentum shell of finite thickness $\Delta M=0.0001$. The Hamilton equations of motion were numerically integrated using a Verlet algorithm with a time step $t_S=10^{-2}$ on the time interval $\tau=2\times10^3$ time units. With values of $m(^{40}\mathrm{Ar})=39.945$ amu, $U_0=99.55$ $\mathrm{cm}^{-1}$, and $\alpha=3.757/2^{1/6}$ Å, the time unit $(m\alpha^2/U_0)^{1/2}=1.94$ ps, the time step $t_S=19.4$ fs, and the time interval $\tau=3.88$ ns. The absolute drift in numerical values of $E_{\rm tot}$ and $M$ on the interval $\tau$ did not exceed $10^{-5}$ and $10^{-7}$, respectively.

For a given value of $E_{\rm tot}$ and $M=|\mathbf{M}|$, a set of 50 to 100 trajectories was used. For each trajectory the maximum Lyapunov exponent $\sigma$, the autocorrelation function $B_p(\tau)=\langle p_i(t+\tau)p_i(t)\rangle$ of the momentum $p_i(t)$ of the $i$th atom on the axis normal to **M**, and the distribution functions of the triangle area, the interatomic distances, and the kinetic and potential energies were calculated. The maximum Lyapunov exponent was calculated by the scheme of Benettin *et al.* [20]. We note that there are two distinct axes normal to **M**; both were used in preliminary calculations of $B_p(\tau)$, but since the results were identical, only one was used subsequently.

## III. RESULTS

Our results cover a wide range of total energies, namely $-2.5$, $-2.3$, $-1.5$, $-1.4$, and $-1.2$, that is, from just above

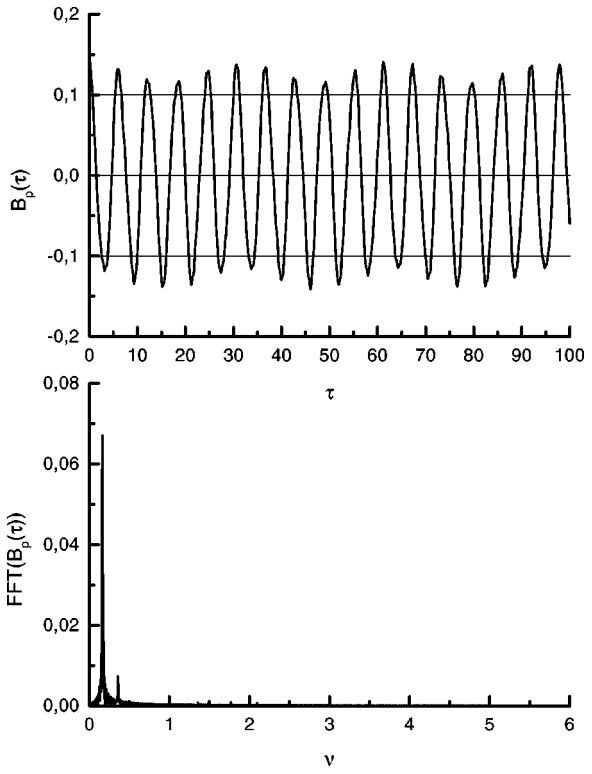


FIG. 2. Typical autocorrelation function $B_p(\tau)$ and its Fourier transform FFT$[B_p(\tau)]$ for regular trajectories with equal distributions of interatomic distances with $E_{\rm tot}=-2.3$, $M/M_{\rm max}=0.8$. The time unit $\tau$ is 1.94 ps (see text), while the frequency unit $\nu$ is its reciprocal of 0.515 THz.

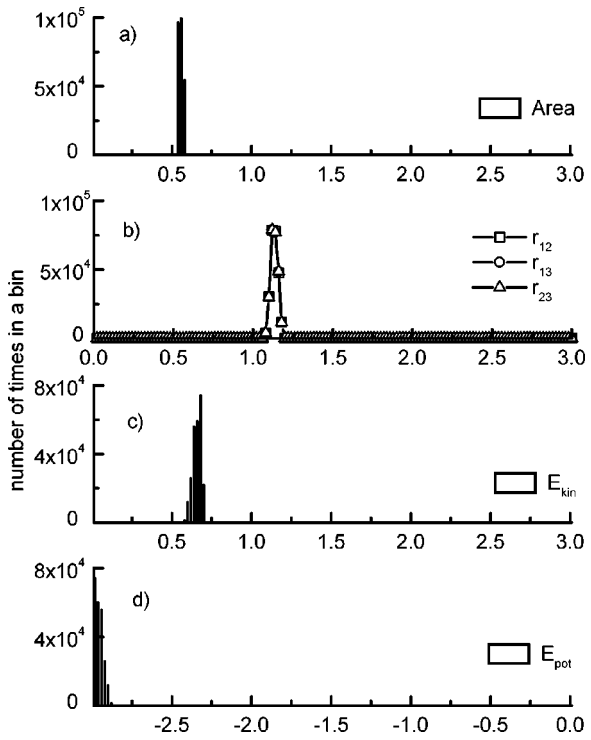


FIG. 3. Histograms for the distribution of (a) the molecular triangle area, (b) interatomic distances, (c) kinetic energy, and (d) potential energy for regular trajectories with $E_{\rm tot}=-2.3$ and $M/M_{\rm max}=0.8$. The area unit in (a) is the square of the diatomic equilibrium separation of 3.757 Å, the distance unit in (b) is the diatomic equilibrium separation of 3.757 Å, and the energy unit in (c) and (d) is the diatomic well depth of 99.45 $\rm cm^{-1}$.

the ground vibrational level at approximately $-2.56$ [21] (the classical minimum potential energy is $-3.0$) to a value close to the dissociation threshold of $-1.0$ to form $Ar_2+Ar$. These selected energies fall into two ranges, one ($-2.5\leqslant E_{\rm tot}\leqslant -2.3$) representing dynamics in the potential-energy well corresponding to predominantly triangular structures and the other ($-1.5\leqslant E_{\rm tot}\leqslant -1.2$) representing dynamics above the linear saddle-point energy. The present results complement our earlier results [14] for $E_{\rm tot}=-1.5$. Three types of trajectories may be identified. These are as follows.

(a) Trajectories with the maximum Lyapunov exponent $\sigma\leqslant(1.0\pm0.3)\times10^{-3}$ for the regular region.

(b) Trajectories with the maximum Lyapunov exponent $\sigma=0.7\pm0.3$ for the chaotic region.

(c) Trajectories with the maximum Lyapunov exponent $\sigma\approx0.2\pm0.05$ for the so-called weakly chaotic region.

A special feature of the phase-space structure is the nonmonotonic dependence of the fraction of phase space filled by regular trajectories as a function of the angular momentum for a given total energy (Fig. 1). The results may be described in terms of two energy regions, the first being from the bottom of the well up to the critical energy $E_{\rm lin}=-2.03$, which permits passage though the linear saddle point, and the second from $E_{\rm lin}$ up to the dissociation limit of $-1.0$.

The lowest energy considered is $-2.5$. At this energy for a nonrotating cluster only a small fraction of the trajectories are found to be regular, indicating that chaotic behavior is obtained even at very low energies, confirming previously reported [21] results. At yet higher energies no regular trajectories are found for the nonrotating cluster, reflecting the anharmonic nature of the potential energy.

Inclusion of rotation leads to the redistribution of internal energy between internal degrees of freedom. As seen in Fig. 1, the introduction of a small angular momentum leads to the disappearance of the regular component since the rotation can deflect the small amplitude atomic oscillations. However, the regular component reemerges at higher angular momenta. When the angular momentum is near the maximum value $M_{\rm max}$ possible for a given total energy the cluster becomes a quasirigid centrifugally distorted rotor, with a large fraction of regular motion.

When $E_{\rm tot}\geqslant E_{\rm lin}$, a nonmonotonic behavior of the regular component appears for large $M=|\mathbf{M}|$ (Fig. 1). It was previously suggested [14] that such behavior reflects the regularizing influence of the linear configuration and the freezing of internal energy into rotational degrees of freedom as $M$ approaches its maximum value for a given total energy. The dashed lines in Fig. 1 simply highlight the nonmonotonic character of the results. The error bars show uncertainties in the fraction of regular trajectories as estimated by $\Delta\mu=(100\mu/N)^{1/2}$, where $N$ is the number of trajectories considered for a given $E_{\rm tot}$ and $M$.

The vertical line in Fig. 1 at a value of $M/M_{\rm max}=0.837$ corresponds to the value of the normalized angular momen-

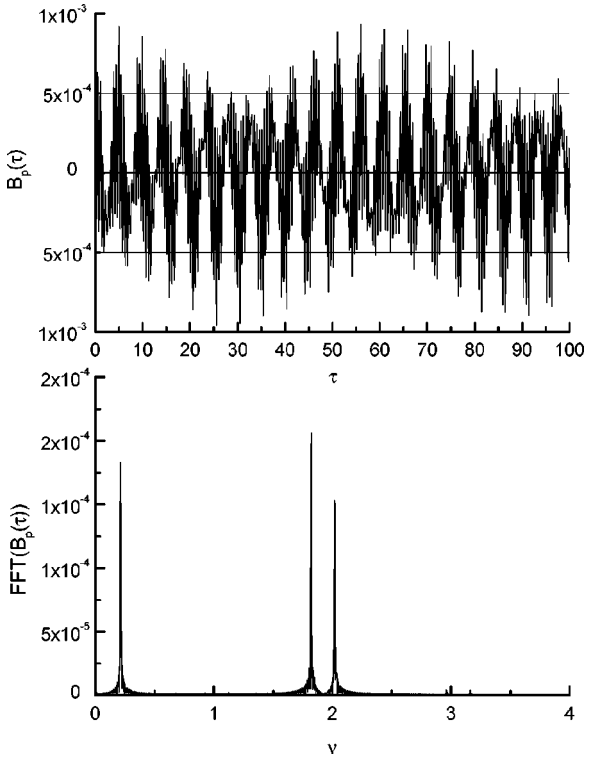


FIG. 4. Typical autocorrelation function $B_p(\tau)$ and its Fourier transform FFT$[B_p(\tau)]$ for regular trajectories with equal distributions of interatomic distances with $E_{\mathrm{tot}}=-1.5$ and $M/M_{\mathrm{max}}=0.8$. The time unit $\tau$ and the frequency unit $\nu$ are as in Fig. 2.

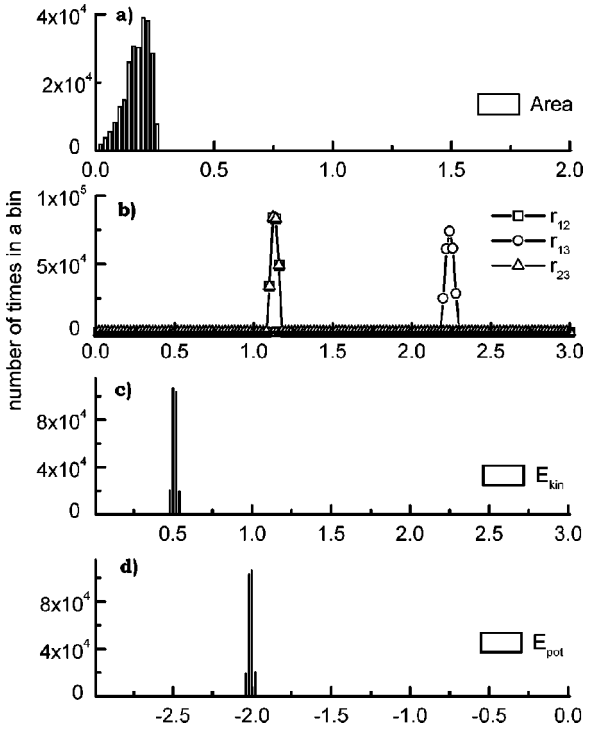


FIG. 5. Histograms for the distribution of (a) the molecular triangle area, (b) interatomic distances, (c) kinetic energy, and (d) potential energy for regular trajectories with $E_{\mathrm{tot}}=-2.3$ and $M/M_{\mathrm{max}}=0.8$. The units of area, distance, and energy are as in Fig. 3.

tum for a nonvibrating linear structure with a total internal energy of $-1.5$, for which the angular momentum is a maximum for a nonvibrating equilateral triangular structure with **M** aligned along its $C_3$ axis. That is, the angular momentum for a nonvibrating linear structure with this energy is less by a factor of 0.837. This factor depends sensitively upon the total energy, rising from zero at the threshold of $-2.031$ for the linear structure to 0.957 at an energy of $-1.2$, the highest energy value considered here, and exceeds unity for slightly higher energies. For a value of $M/M_{\mathrm{max}}$ greater than the value of this factor at a fixed total energy the structure cannot be linear. Indeed we see in Fig. 1 for an energy of $-1.5$, for which this factor is 0.837, that the fraction of regular trajectories begins to fall as $M/M_{\mathrm{max}}$ exceeds a value of approximately 0.75. Similarly, a nonvibrating acute isosceles triangular structure with a total energy of $-1.5$ and with **M** aligned along its $C_2$ axis has a value of $M/M_{\mathrm{max}}=0.723$, only slightly larger than the ratio of $2^{-1/2}=0.707$ for a rigid rotor. This ratio is relatively insensitive to the energy, rising from 0.711 to 0.730 as the total energy increases from $-2.5$ to $-1.2$. For a value of $M/M_{\mathrm{max}}$ greater than this factor at a fixed total energy the angular momentum vector **M** is forced out of the molecular plane. For total energies between $-2.031$ and $-1.685$, linear structures are excluded with increasing $M$ before those with **M** aligned along a $C_2$ axis, while for energies above $-1.685$ the latter are excluded before the former. In either case the accessible configuration and orientation spaces shrink as $M/M_{\mathrm{max}}$ increases to unity. This shrinking is accompanied by a reduction in the spread of possible vibrational energies, corresponding to the difference between the maximum and minimum values of the rotational energy for a given total energy and magnitude of **M**. This spread is a maximum when $M$ is such that there is zero vibrational energy for **M** lying in the molecular plane (a quasirigid rotor), but nonzero for **M** out of the plane.

We may now use the concepts outlined above to interpret further the key results presented in Fig. 1. For each of the four values of $E_{\mathrm{tot}}$ considered the percentage $\mu$ of regular trajectories is nearly zero until $M/M_{\mathrm{max}}$ reaches a value around $2^{-1/2}=0.707$ such that **M** is excluded from the molecular plane. If we view **M** as fixed in the laboratory frame this means that orientational disorder (tumbling) is reduced as $M/M_{\mathrm{max}}$ is increased further. For $E_{\mathrm{tot}}$ values of $-2.5$ and $-2.3$ linear configurations are not accessible. For $E_{\mathrm{tot}}=-1.5$ linear configurations are accessible but only up to $M/M_{\mathrm{max}}=0.837$, around which $\mu$ falls. Similarly for $E_{\mathrm{tot}}=-1.2$ linear configurations are accessible up to $M/M_{\mathrm{max}}=0.957$, around which $\mu$ falls (not shown). Linear configurations have a minimum of 0.969 units of stored internal potential energy, so that their exclusion permits an increased fraction of chaotic trajectories associated with low potential energies and high kinetic energies.

For the regular component with maximum Lyapunov exponent $\sigma\leqslant(1.0\pm0.3)\times10^{-3}$ two kinds of trajectories have been found. These are distinguished by the shapes of their autocorrelation functions, the number of harmonics in their Fourier spectra, and their distributions of dynamical variables. The first regular kind is a quasirigid rotation of $Ar_3$

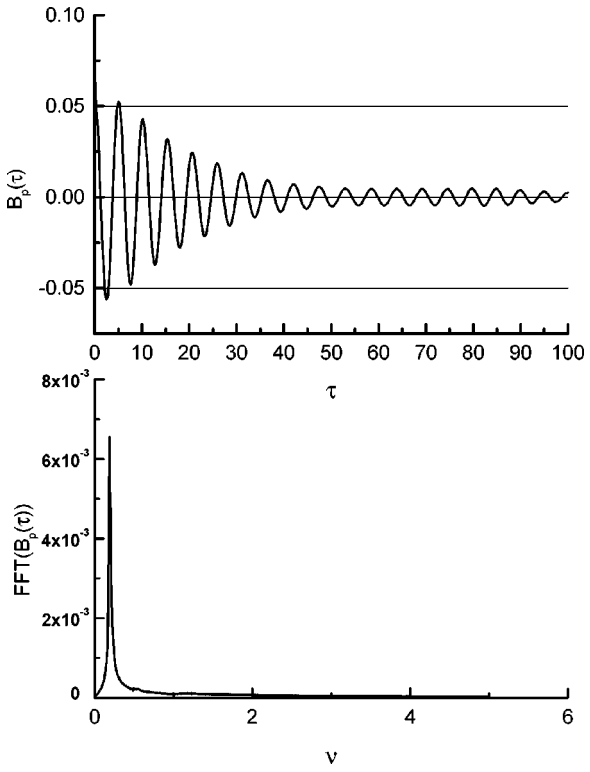


FIG. 6. Typical autocorrelation function $B_p(\tau)$ and its Fourier transform FFT$[B_p(\tau)]$ for the strongly chaotic component at $E_{\rm tot}=-1.4$ and $M/M_{\rm max}=0.8$. The time unit $\tau$ and the frequency unit $\nu$ are as in Fig. 2.

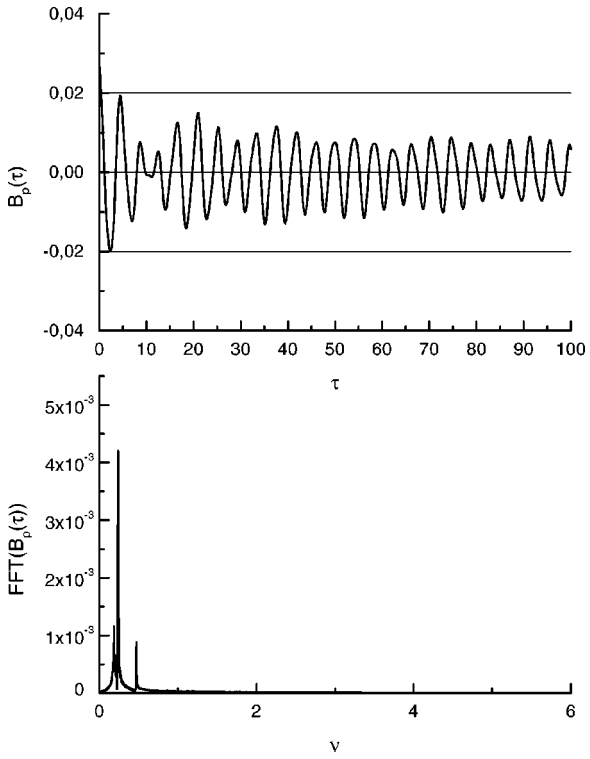


FIG. 7. Typical autocorrelation function $B_p(\tau)$ and its Fourier spectrum FFT$[B_p(\tau)]$ for the weak chaotic component $E_{\rm tot}=-1.4$ and $M/M_{\rm max}=0.8$. The time unit $\tau$ and the frequency unit $\nu$ are as in Fig. 2.

with a unimodal autocorrelation function (Fig. 2) and equal distributions of interatomic distances (Fig. 3). Another regular kind is characterized by a multimodal autocorrelation function with its multiharmonic Fourier spectrum (Fig. 4) and two equal distributions of interatomic distances (Fig. 5). These distributions have two narrow maxima at $r_{ij}\simeq 2^{1/6}$ and one at $r_{ij}\simeq 2\times 2^{1/6}$, connecting this type of regular motion with quasinormal vibrations of a nearly linear cluster.

The differences in the two kinds of regular motions are reflected in Fig. 3 for $E_{\rm tot}=-2.3$ and Fig. 5 for $E_{\rm tot}=-1.5$. The potential-energy distribution has a narrow peak centered near the bottom of the well for the former but near the linear saddle point for the latter. This result confirms our suggestion that for $E_{\rm tot}>-2.0$ and $M\leqslant M_{\rm lin}$, where $M_{\rm lin}$ is the maximum possible value of $M$ for a linear structure with a given value of $E_{\rm tot}$, the motion of the trimer through its linear configuration regularizes the trajectories. The disappearance (Fig. 1) of regular trajectories for $E_{\rm tot}>-2.03$ is accounted for by the inaccessibility of the linear configuration when $M$ is greater than $M_{\rm lin}(E_{\rm tot})$. The only mechanism that can regularize the motion under these conditions is quasirigid rotation, which appears as $M\rightarrow M_{\rm max}(E_{\rm tot})$. Initial conditions with $M=M_{\rm max}(E_{\rm tot})$ are a rare occurrence and thus do not contribute to the fraction of regular trajectories in Fig. 1.

As we previously noted, the chaotic motion is split into two long-lived and, for some energies, nonoverlapping components that differ in their maximum Lyapunov exponents. Typical autocorrelation functions and their Fourier spectra

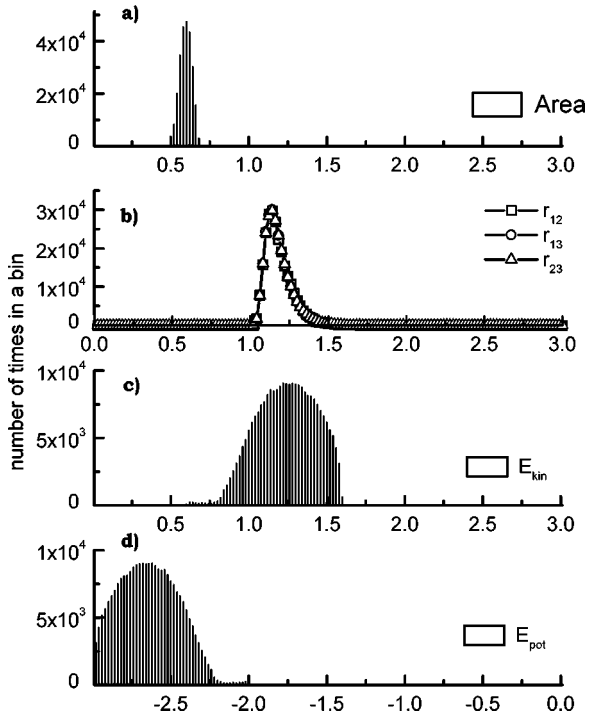


FIG. 8. Histograms for the distribution of (a) the molecular triangle area, (b) interatomic distances, (c) kinetic energy, and (d) potential energy for strongly chaotic trajectories with $E_{\rm tot}=-1.4$ and $M/M_{\rm max}=0.8$. The units of area, distance, and energy are as in Fig. 3.

for the strongly and weakly chaotic components are shown in Figs. 6 and 7, respectively. The autocorrelation function decay times, which are related to the maximum Lyapunov exponents and which may be taken as a time scale for internal energy randomization [2], differ for the two components. Because of the existence of trajectories with long-time correlations (weak chaotic components) it is natural to suppose that rotation plays an unimportant role if energies are above the dissociation level.

Typical distributions for the dynamical variables for the strong chaotic component are shown in Fig. 8. At a given total energy and angular momentum the interatomic distances have identical broad distributions covering all accessible values, leading to a broad distribution in the area of the cluster triangle. We also note from the distributions of potential and kinetic energies that internal energy flows freely between these contributions, reflecting a coupling not present in the regular components of the motion.

## IV. SUMMARY

We have shown that the influence of rotation on the dynamics of the $Ar_3$ van der Waals cluster depends in a nonmonotonic manner on the magnitude of its angular momentum. Regular trajectories exhibiting quasirigid rotation become rare at high internal energies as the concomitant high vibrational kinetic energy is largely responsible for the chaotic motion. Chaos is reduced when the angular momentum becomes sufficiently large for a given total energy that it is excluded from the molecular plane. Regular and weakly chaotic components of the motion arise when the energy permits passage through linear configurations. Chaotic motion, which may be partitioned into strongly and weakly chaotic components, may play an important role at energies above the threshold for dissociation and produce deviations from RRKM behavior. The strongly chaotic component is characterized by strong coupling between potential and kinetic energies.

## ACKNOWLEDGMENTS

The authors would like to thank Dr. P.V. Elyutin for fruitful discussions on the phase-space structure of rotating rare-gas trimers and Mrs. L. Shvilkina for help with computational programs. This work was partially supported by INTAS (Grant No. 96-865). E.D.B. acknowledges Russian Basic Research Foundation (Grant No. 97-03-33766) and the program University of Russia Fundamental Research (Grant No. 5036) for partial support.

[1] R.S. Berry, J. Chem. Soc., Faraday Trans. **86**, 2342 (1990); J. Phys. Chem. **98**, 6910 (1994); Int. J. Quantum Chem. **58**, 657 (1996).
[2] S.C. Farantos, Chem. Phys. Lett. **92**, 379 (1982).
[3] C. Amitrano and R.S. Berry, Phys. Rev. Lett. **68**, 729 (1992).
[4] C. Amitrano and R.S. Berry, Phys. Rev. E **47**, 3158 (1993).
[5] S.K. Nayak, R. Ramaswamy, and C. Chakravarty, Phys. Rev. E **51**, 3376 (1995).
[6] T.L. Beck, D.M. Leitner, and R.S. Berry, J. Chem. Phys. **89**, 1681 (1988).
[7] D.J. Wales and R.S. Berry, J. Phys. B **24**, L351 (1991).
[8] R.J. Hinde, R.S. Berry, and D.J. Wales, J. Chem. Phys. **96**, 1376 (1992).
[9] S.C. Farantos and J.N. Murrell, Chem. Phys. **55**, 205 (1981).
[10] S.C. Farantos, J. Phys. Chem. **87**, 5061 (1983).
[11] V.I. Arnol'd and A. Avez, *Ergodic Problems in Classical Mechanics* (Benjamin, New York, 1968).
[12] J. Jellinek and P.G. Jasien, in *The Structure of Small Molecules and Ions*, edited by R. Naaman and Z. Vager (Plenum, New York, 1988), pp. 39–47.
[13] N. Fahrer and C. Schlier, J. Chem. Phys. **97**, 7008 (1992).
[14] E.D. Belega, P.V. Elyutin, D.N. Trubnikov, and L.B. Shvilkina, (unpublished); Phys. Dokl. **355**, 750 (1997).
[15] P.V. Elyutin, V.I. Baranov, E.D. Belega, and D.N. Trubnikov, J. Chem. Phys. **100**, 3843 (1994).
[16] E. Yurtsever, Europhys. Lett. **37(2)**, 91 (1997).
[17] E. Yurtsever and N. Elmaci, Phys. Rev. A **55**, 538 (1997).
[18] E. Yurtsever, Phys. Rev. A **58**, 377 (1998).
[19] W.D. Kristensen, E.J. Jensen, and R.M. Cotterill, J. Chem. Phys. **60**, 4161 (1974).
[20] G. Benettin, L. Galgani, and J. Strelcyn, Phys. Rev. A **14**, 2338 (1976).
[21] D.M. Leitner and R.S. Berry, J. Chem. Phys. **91**, 3470 (1989).